Inner Volume MR Imaging: Technical Concepts and Their Application[1]

David A. Feinberg, Ph.D.
John C. Hoenninger, M.S.E.E.
Lawrence E. Crooks, Ph.D.
Leon Kaufman, Ph.D.
Jeffrey C. Watts, M.S.
Mitsuaki Arakawa, B.S.

Although cross-sectional magnetic resonance examination of the head and body is useful for screening large regions of tissue, subsectional regions of the head and body often need to be examined. Orthogonally directed, selectively irradiated planes with different flip angles produce a spatially limited signal region from which two- or three-dimensional volume images can be reconstructed. Images with limited fields-of-view can be acquired in reduced imaging time. We present a general description of this technique. These subsectional or "inner volume" images eliminate respiratory motion artifacts by excluding moving tissues from the imaged volume. A result of this technique is a high signal from rapid pulsatile blood flow, produced without cardiac gating the pulse sequence.

Index terms: Blood, flow dynamics • Brain, magnetic resonance studies, 13.1299 • Heart, magnetic resonance studies, 51.1299 • Magnetic resonance, technology

Radiology 1985; 156:743–747

In magnetic resonance (MR) Fourier imaging, the size of the phase-encoded dimensions from which MR signal is produced must be less than the imaged field-of-view; otherwise, signal located outside the field-of-view is aliased into lower frequencies. When the object is too large, the lower frequencies fold over onto existing object frequencies, and two regions of tissue become superimposed (Fig. 1). In whole-body MR imaging, this problem is avoided by either reducing the spatial resolution or by increasing the number of image lines to extend the field-of-view beyond the boundaries of the body. Alternatively, if the extent of the signal volume could be spatially limited to a smaller region of the body, the field-of-view can be reduced without the problem of aliasing. Surface coils may be used to reduce the extent of the signal volume by localizing the radiofrequency (RF) sensitivity close to the surface of the body; inner regions of the body, however, will provide only weak signals.

We describe an MR imaging method that selectively images inner regions of the body without imaging adjacent surrounding tissue present in the whole body cross section. The imaging time can be reduced proportionate to the reduced field-of-view. In one application, inner volume MR imaging could be used to exclude from images the moving regions of the body that produce severe artifacts in regions of interest. For example, in MR body images, artifacts caused by the respiratory motion of the abdominal wall can be removed from images of the spine. In a different application, inner volume images could be used to assess flow in blood vessels deep within the body when it is not necessary to image adjacent static tissue.

The imaging time required to define an inner volume is directly proportional to the number of image lines multiplied by the number of image sections (Table 1). The time required to image an entire body cross section at coarse spatial resolution can instead be spent defining a narrower region with higher spatial resolutions, since the problem of aliasing is eliminated by this technique. The imaging time saved by reducing the field-of-view on one spatial axis can also be spent defining multiple image sections or encoding blood flow, chemical shift, or other physical parameters in the region of interest.

MATERIALS AND METHODS

Similar to earlier MR selective line-scan imaging techniques (1, 2), inner volume imaging uses two or more spatially selective RF pulses to excite and invert nuclei in two perpendicular volumes (Fig. 2). The intersecting volume of tissue first has its spins nutated by 90° and then by 180° to produce a spin-echo signal for image reconstruction. The image volume can be positioned electronically anywhere within the body.

To produce two-dimensional (2D) Fourier transform images, multiple cycles of the pulse sequence encode the phase of the signal to spatially resolve information along one axis (Appendix). A signal readout gradient applied on a second perpendicular axis gave the second dimension of in-plane spatial resolution (3). To produce a three-dimensional (3D) image, the

[1] From the Department of Radiology, University of California San Francisco. Received February 28, 1985; accepted and revision requested April 29; revision received May 8. Research supported by Diasonics Inc., MRI Division.

above multicycle sequence is repeated in its entirety with additional phase encoding along the third axis orthogonal to the image plane (Fig. 3) as many times as there are sections (3–5). In these experiments, eight sections were defined. For both the 2D and 3D images, the in-plane spatial resolution was 1.7 × 1.7 mm. The section thickness of the 2D images were 7 mm, and the 3D image sections were 5 mm thick.

Inner volume images were positioned onto target regions by displacement of one of the two RF pulse planes (Fig. 2). Initially, the pulse sequence was calibrated to determine the spatial displacement on each axis per frequency offset (cm/Hz). The resulting scale factors were used in all the experiments to position the inner volume images onto regions of interest. For 3D volume imaging, a 2D inner volume image of the body or head was first acquired to find the coordinates of the arteries or target structures with respect to the center of the image. The coordinates were converted to frequency offsets for positioning the 3D inner volume image.

Experiments were conducted on a prototype Diasonics MT/S whole-body imaging system (Milpitas, Calif.) that included a superconducting magnet operating at 0.35 T and equipped with three orthogonal sets of gradient coils. The patient lies on a bed having variable positions parallel to the direction of the static magnetic field, defined as the z-axis. The vertical direction and horizontal direction are defined as the y-axis and x-axis, respectively. Synchronization of the pulse sequence to the subject's cardiac cycle was made possible with a battery-powered electrocardiogram monitor having three leads connected to the subject's chest. A fiber-optic cable transferred the ECG signal out of the magnet and RF screen room enclosure. The transduced signal was connected to the system's control computer with an intermediate trigger delay used by the operator to set a temporal delay between the ECG R-wave and the beginning of each pulse sequence cycle.

Table 1
Inner Volume Pulse Sequence Data

Physical Dimensions	Imaging Time	Relative S/N
1D, spatial	n·TR	$\sqrt{n}/V$
2D, spatial	P·n·TR	$\sqrt{(nP)}/V$
3D, spatial	P·n·S·TR	$\sqrt{(nPS)}/V$
2D, multisection	P·n·TR	$\sqrt{(nP)}/V$

Note.—TR = repetition time of pulse sequence, P = the number of phase-encoded cycles of the sequence, n = the number of redundant signals used for averaging, V = the image element volume or voxel dimension, and S = the number of image sections.

RESULTS

Figure 4 shows three 2D inner volume images of the brain acquired with 64, 32, and 16 lines and obtained at the same positions as the aliased images in Figure 1. The three images in Figure 4 had the same resolution, section thickness, and number of signal averages (n = 4) and were acquired with a TR = 0.25 seconds. The respective imaging times were 2, 1, and 0.5 minutes, compared with 4 minutes for a full cross section, for fields-of-view of 25.6, 12.8, 6.4, and 3.2 cm. The respective signal-to-noise ratios (S/N) measured in white matter were 47.4, 35.2, 26.1, and 16.7, showing improvement with the square root of imaging time and consistent with the predicted relative S/N in Table 1. The higher value of S/N of the full volume can be obtained with 3D inner volume imaging if the imaging time is held constant and the number of sections is increased by the same factor that is used to decrease the number of lines. (Data acquisition time = number lines × number of sections × TR × number of signals averaged, where TR = repetition time.)

Sagittal images of the thoracic spine were made with cross-sectional, 2D, spin-echo imaging (Fig. 5a) and with 2D inner volume imaging (Fig. 5b). The abdominal chest wall, undergoing normal breathing motion, produced noticeable crescent-shaped artifacts in the cross-sectional image with full field-of-view. No artifacts were noticeable in the inner volume image. Transverse images of the abdomen (Fig. 6) showed similar elimination of breathing artifact.

Transaxial 3D inner volume images of a human heart (Fig. 7) were acquired with 64 lines and eight sections. The imaging time per section was half that required to image similarly the entire cross section of the body requiring 128 lines. The image volume was intentionally positioned inside the thoracic cavity to exclude the breathing motion–dependent signal of subcutaneous fat from the images. Respiratory gating is sometimes used to eliminate these artifacts, even though it extends imaging time (6).

To visualize blood flow in the cranial vessels, 3D volume images were made with eight sections and 32 lines, TR = 0.25 seconds, n = 4, and image acquisition time of 4 minutes. Relatively high signal magnitude compared with surrounding static tissue was observed in the internal carotid arteries in both the first and second echo images, as well as in the vertebral arteries and jugular veins (Fig. 8). These images of rapidly flowing pulsatile blood were made without synchronization of the pulse sequence to the cardiac cycle (cardiac gating).

DISCUSSION

When imaging the spine and other organs where artifacts are caused by breathing motion, gating a pulse sequence to the respiratory cycle is effective in reducing these artifacts (6). With respiratory gating, however, intrinsic variation in TR would occur if data were taken immediately after each restart, and longer imaging time is necessary because of the delays during which data is not acquired. The cross-sectional image of the spine that included chest wall showed a much

Figure 1

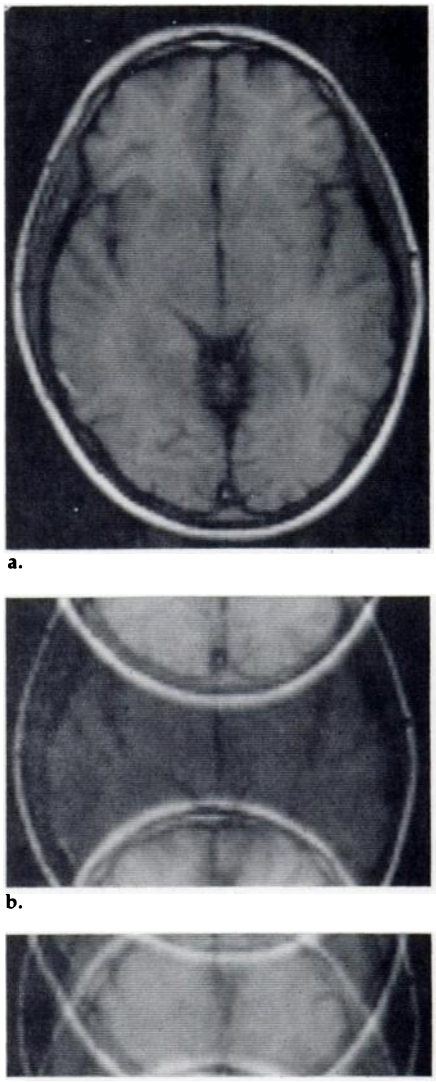

Demonstration of aliasing in conventional 2D image with coplanar 90° RF pulse and 180° RF pulse. In general, the field-of-view = the number of image lines × the spatial resolution on the same axis.

a. Cross-sectional image with image field-of-view greater than the extent of the signal producing region with 128 image lines. The field-of-view is reduced to less than the signal extent either by increasing the spatial resolution or by decreasing the number of image lines.
b. Regions of the head outside the field-of-view are aliased into opposite ends of the image when 64 image lines are used.
c. Further superposition of tissue volumes occurs with greater reduction in field-of-view using 32 image lines.

Figure 2

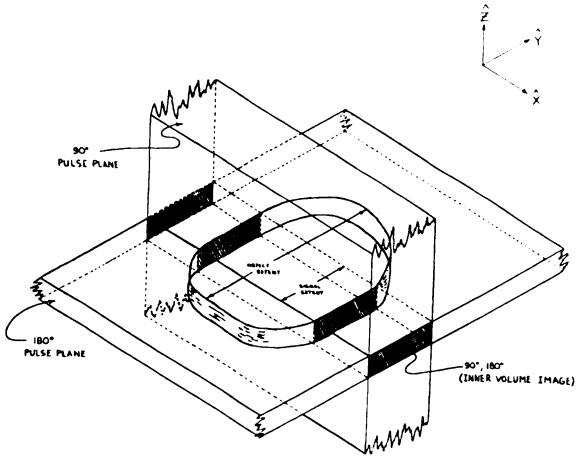

Method of producing spin-echo signal in the intersecting region of the two spatially selective irradiations. A 90° RF pulse excites nuclei within a planar volume (broken or jagged lines indicate continued region), and the subsequent 180° RF pulse inverts the nuclei in a planar volume perpendicular to the first plane. Only those spin nuclei that experience both the 90° excitation pulse and the 180° inversion pulse are refocused to produce a spin-echo signal. With the signal extent reduced to less than the object extent, a correspondingly narrower image field-of-view is permitted without superposition of outer regions onto the inner region of the image.

Figure 3

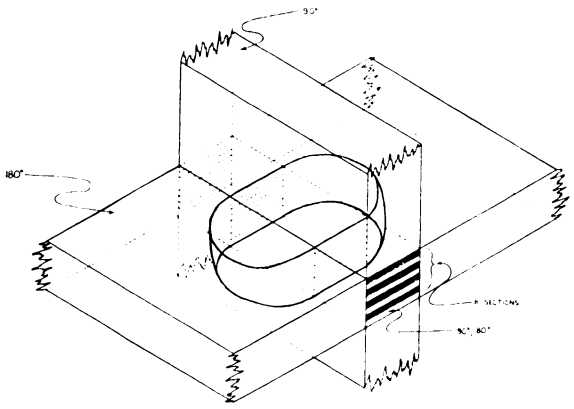

To produce 3D inner volume images, the 180° RF pulse irradiates a thicker region of tissue. Independent phase encoding along the z-axis permits resolution of the image sections within the thicker volume.

Figure 4

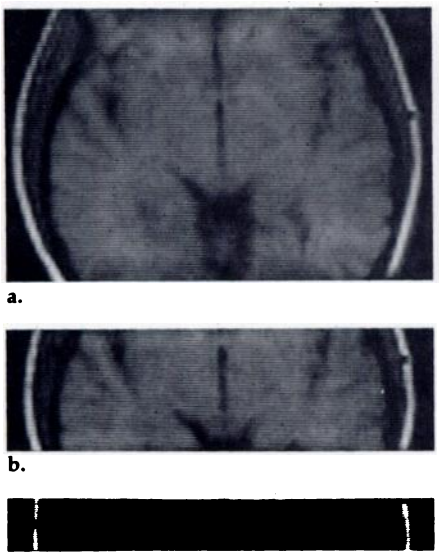

a.

b.

c.

Inner volume 2D images of the head using 64 lines (**a**), 32 lines (**b**), and 16 lines (**c**) are at the same position as Fig. 1 and at the same spatial resolution (1.7 × 1.7 mm) and section thickness (7 mm). Inner volume images are made by reducing the extent of the signal-producing region. The thickness of the 180° RF pulse plane of Fig. 2 is set equal to the in-plane field-of-view, while the 90° RF pulse plane determines the section thickness. Unlike images in Fig. 1, signal is not generated in the outer regions of the head, which are irradiated by the 180° pulse but not by the 90° pulse.

Figure 5

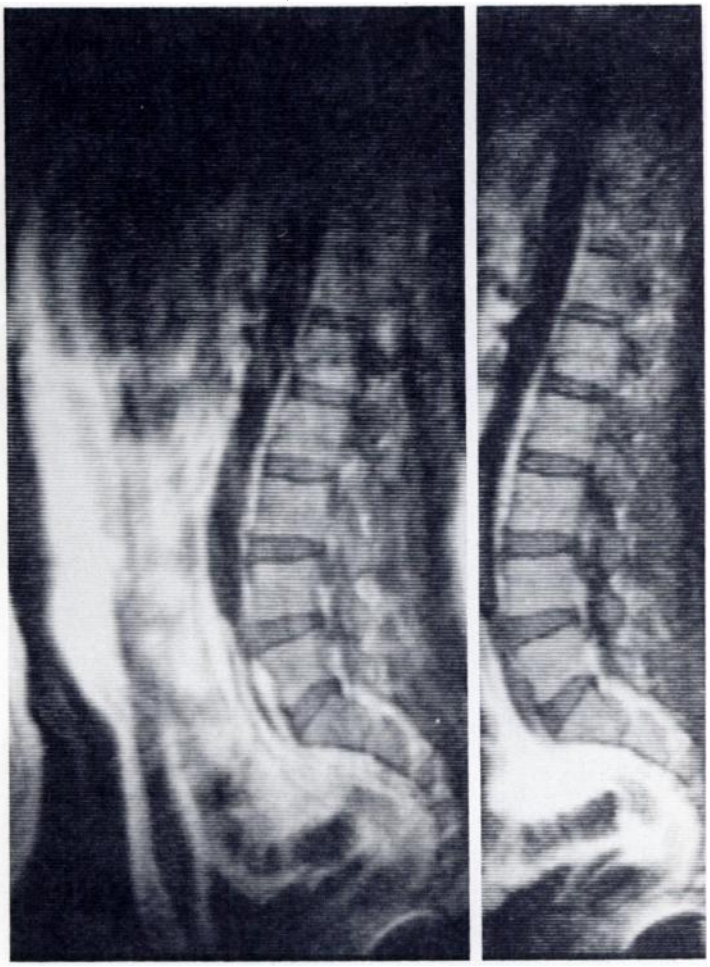

a. b.

Full cross-sectional sagittal image of spine shows typical artifacts on spine (**a**) while the inner volume image (**b**) does not show artifacts.

higher level of vertical band artifacts than observed in the inner volume image. This artifact can largely be attributed to the motion of fat, which

Figure 6

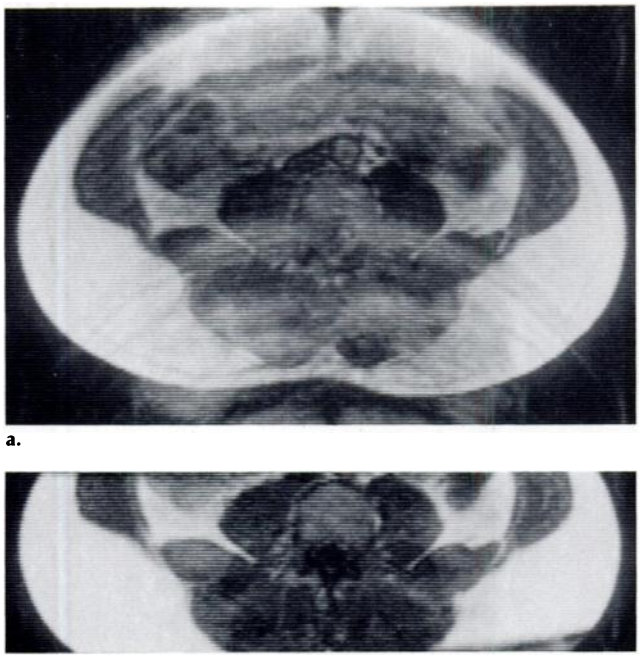

a.

b.

Transverse image of the abdomen (**a**) with entire cross section of body and inner volume image (**b**) located below the abdominal wall.

Figure 7

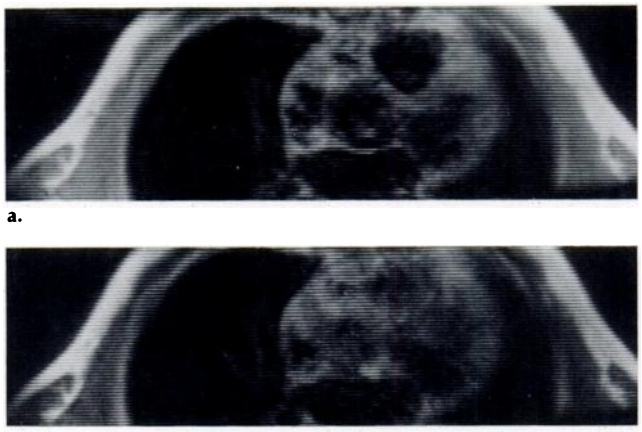

a.

b.

Three-dimensional inner volume images of the heart obtained with cardiac gating including a first spin-echo image at TE = 28 msec (**a**) and a second echo image at TE = 56 msec (**b**). Spatial resolution is 1.7 × 1.7 × 5 mm.

Figure 8

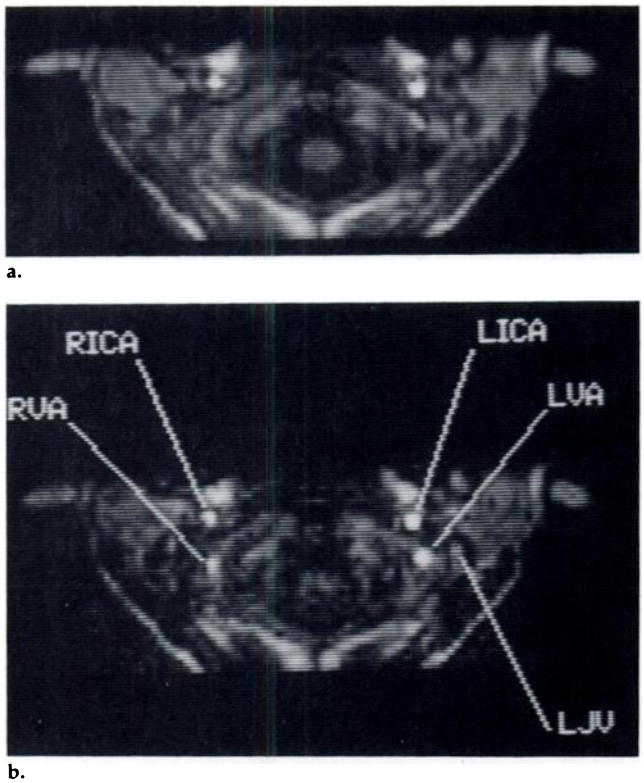

a.

b.

Three-dimensional inner volume images of the head show left and right internal carotid arteries (*ICA*), vertebral arteries (*VA*), and jugular veins (*JV*). The first echo image (**a**) and second echo image (**b**) show high signal magnitude of blood during pulsatile flow without synchronization of the image sequence to the cardiac cycle. Spatial resolution is 1.7 × 1.7 × 5 mm.

has high signal magnitude and which changes position during respiratory expansion of the chest. The position of the fat is not the same in each cycle of the pulse sequence, and therefore it produces deviations from the otherwise linearly increasing phase-encoding process.

With our 2D, multisection MR imaging, blood flowing at a high velocity produces very low signal because of the effect of magnetic gradients on the phase of moving nuclei, and because blood flows out of the section during the process of spin-echo creation (7). The visualization of unusually high signal from rapidly flowing blood (Fig. 8) can be understood with respect to the above two factors. Regardless of the velocity of the upstream blood on the z-axis or position in the excited volume, the 180° pulse always refocuses some of the blood to produce a spin-echo signal. The blood centered on position $z = -V_z/(TE/2)$ upstream from the 180° RF plane and where TE = echo time, is refocused to produce a spin-echo signal (Fig. 9). Although blood flowing at low velocity and high velocity experiences the 90° pulse at different positions upstream in these nongated studies, both can produce spin-echo signal. In general, the combined pulse sequence TR, vessel length and direction, heart rate, pulsatile changes in velocity, and image volume dimensions all directly affect the signal magnitude from blood in each cycle of the pulse sequence.

Also, nuclei moving in the direction of a magnetic gradient undergo a change in phase proportional to their velocity. If a distribution of velocities exists within a voxel, then an incoherent signal results with reduced mag-

Figure 9

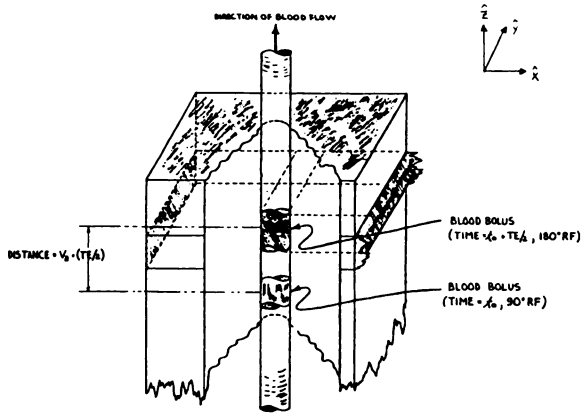

Pulsatile blood flow directed along the z-axis orthogonal to the image plane. The 90° RF pulse is on the long axis of the vessel and irradiates all the blood within the nonselective volume. The 180° pulse refocuses the blood bolus, which was irradiated by the 90° pulse upstream and outside of the inner volume region.

Figure 10

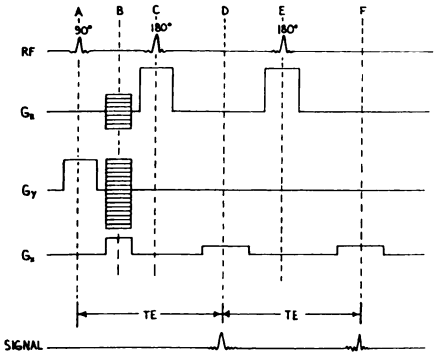

Imaging sequence of 3D inner volume image having transaxial orientation.

nitude. In the 3D inner volume images, the 90° selective excitation uses a gradient applied perpendicular to the direction of flow, and consequently the net phase of the flowing nuclei is unaffected by the gradient. It is possible to develop different permutations of the inner volume pulse sequence by applying the volume-selective gradient pulses on different axes. For example, swapping section-selective y and z gradients in Figure 2 would produce a completely different signal dependence on flow.

CONCLUSION

A new method for MR imaging subvolumes of objects or of body tissues has been presented. The positive contrast of blood in cranial vessels with rapid pulsatile flow indicates that inner volume imaging may find a diagnostic niche in cardiovascular imaging, augmented by its fast imaging time. These experiments demonstrate a new method for eliminating respiratory motion artifacts from a region of stationary tissue adjacent to moving tissue. ■

Acknowledgment: The authors express their graditude to Gary Temkow for his graphic design of illustrations.

Send correspondence and reprint requests to: David A. Feinberg, Ph.D., University of California San Francisco, Radiologic Imaging Laboratory, 400 Grandview Drive, South San Francisco, California 94080.

APPENDIX

The imaging sequence shown in Figure 10 produces two spin-echo images with transaxial orientation. The sequence begins when a sinc-modulated 90° nutation RF pulse (*A*) occurs simultaneously with a G_y gradient pulse to produce the spatially selective excitation of nuclear spins. Three gradient pulses (*B*) are applied; G_y phase encodes in-plane resolution, G_z phase encodes image sections, and G_x defocuses the free induction decay (FID) to temporally center the later occurring spin-echo signal. A sinc-modulated 180° RF pulse (*C*) occurs simultaneously with a G_z gradient pulse to produce echo refocusing. A readout gradient G_x frequency encodes (*D*) the spin-echo signal for resolution along an in-plane axis; a second spatially selective refocusing of signal (*E*) produces a second spin-echo signal (*F*). To produce sagittal images, all the gradient pulses G_z and G_x are interchanged.

The 2D images were made by iteration of the pulse sequence each time with a different magnitude of G_y at (B). To produce 3D images, the process is repeated as many times as there are sections, with different G_z linear phase-encoding gradient strengths at (B).

Each of the above described cycles of the pulse sequence can be repeated several times (n) for signal averaging and to cancel FID artifacts. These artifacts afe produced by FID signal active during the spin-echo but generated by the 90° irradiation of the planar region outside the inner volume. Such artifacts can be canceled with two cycles of the pulse sequence by changing the phase of the 180° irradiation so that the FID and spin echo have the same sign in one of the data acquisitions and opposite signs in the other acquisition. The averaging is performed by subtracting the two data sets so that the spin echoes add but the FIDs cancel. An FID can also be generated by regions outside the inner volume exposed to the 180° irradiation where the angle is not precisely 180° because of RF inhomogeneity or the profile of the irradiation. Two more averages where the phase of the 90° irradiation is changed to make the sign of this FID opposite that of the spin echo will allow cancellation of this artifact. Thus, four average imaging eliminates these FID artifacts and improves S/N by a factor of two.

References

1. Garroway AN, Grannell PK, Mansfield P. Image formation in NMR by a selective irradiation process. J Phys Chem 1974; 7:L457.
2. Crooks LE. Selective irradiation line scan techniques for NMR imaging. IEEE Trans Nucl Sci 1980; NS-27:1239.
3. Kumar A, Welti D, Ernst RR. NMR Fourier zeugmatography. J Magnetic Resonance 1975; 18:69–83.
4. Johnson G, Hutchison J, Redpath T, Eastwood L. Improvements in performance time for simultaneous three-dimensional NMR imaging. J Magnetic Resonance 1983; 54:374–384.
5. Crooks LE, Watts JC, Hoenninger JC, et al. Thin section definition off magnetic resonance imaging: technical concepts and their implementation. Radiology 1985; 154:463–467.
6. Schultz CL, Alfidi RJ, Nelson AD, Kopiwoda SY, Clampitt ME. Effect of motion on two-dimensional Fourier transformation magnetic resonance images. Radiology 1984; 152:117–121.
7. Feinberg DA, Crooks LE, Hoenninger J, Arakawa M, Watts J. Pulsatile blood velocity in human arteries displayed by magnetic resonance imaging. Radiology 1984; 153:177–180.